Journal of Applied Research and Technology

www.jart.icat.unam.mx

Journal of Applied Research and Technology 21 (2023) 98-105

Original

Using the linear damage summation hypothesis in determining the endurance limit of titanium alloy

Arkadiy A. Skvortsov • Evgeniya O. Gnatyuk* • Olga Yu. Sklemina • Vladimir K. Nikolaev

Department of Dynamics, Strength and Resistance of Materials, Moscow Polytechnic University, Moscow, Russian Federation

Received 02 18 2021; accepted 01 28 2022
Available 02 28 2023

Abstract: The presented paper is relevant, as it presents the results of fatigue tests of titanium alloy. The purpose of the article is to describe the use of the hypothesis of linear damage summation when processing the results of fatigue tests. In the study, the authors used empirical methods such as indirect observation of the object under study, description, and measurement of technical influences exerted on it by an artificial means. The linear regression analysis to establish the relationship between stress and durability was also used. The endurance limit of the titanium alloy was determined, which lies in the range from 460 to 480 MPa with the number of cycles from 105 to 108. It was concluded that the use of the linear damage summation hypothesis in processing the results of fatigue tests entails a satisfactory practical accuracy of the calculation of endurance limit

Keywords: regression analysis, technical titanium, crack, loads, strain energy

*Corresponding author.
E-mail address: evgeniyagnatyuk0@gmail.com(Evgeniya O. Gnatyuk).
Peer Review under the responsibility of Universidad Nacional Autónoma de México.

1. Introduction

It is commonly known that under the action of cyclic stresses in metals and alloys, cracks appear and gradually develop, ultimately causing destruction. Such processes of gradual accumulation of damage under the influence of cyclic loads are called fatigue. Fatigue fractures are especially dangerous in that they can develop under the action of stresses that are much lower than the ultimate strength and yield strength (Borisov et al., 1987; Stepnov, 1985; Suleimenov et al., 2022). It is noted that more than 80% of all cases of operational failure occurs as a result of cyclic loading (Bekbauov et al., 2017; Korzhyk et al., 2021; Lei et al., 2021). Due to the long duration, and, consequently, the high cost, fatigue tests to determine the endurance limit of samples are often carried out not until destruction, but for the determination of operating time, a certain test base N_B. In this case, the pieces that have passed the test without destruction are tested again at higher levels of vibration stresses (Grigorenko et al., 2020; Kunanbayeva et al., 2022; Mukhambetzhanov & Baishemirov, 2013). As a rule, when conducting regression analysis of test results, specimens that failed during test with operating time corresponding to N_B are taken into account.

In linear regression analysis to establish the relationship between stress and durability, it is necessary to transform the values in order to represent the equation of the fatigue curve as a linear relationship between the converted values (Borisov & Korzhyk, 1998; Gates & Fatemi, 2017). The following is usually taken as a random variable: $y = lgN$, since it is in this case that the normal distribution law underlying the regression analysis is satisfactory. The transformed value $x = F(\boldsymbol{\sigma a})$ is selected as an independent value. The form of the function $x = F(\boldsymbol{\sigma a})$ is set so that the dependence $y = f(x)$ is linear (Kvasnytskyi et al., 2020; Razavi et al., 2020; Shojaei & Volgers, 2017). The fatigue curve equation has the form:

$$Y = a + b(x - \bar{x}) \tag{1}$$

where: $x = lg\boldsymbol{\sigma}$; $y = lgN$; a and b – fatigue curve parameters.

With an insufficient amount of fatigue tests, the parameters of Equation (1) are determined on the basis of regression analysis, the equation of the averaged fatigue curve corresponding to the fracture probability $P = 0.5$ is established. With a sufficient amount of testing, a family of curves can be constructed for a number of fixed levels of fracture probabilities (Kunitskii et al., 1988, 1990; Panfilov et al., 2020; Rege et al., 2019). For the experiments, an alloy of technical titanium was used, intended for the manufacture of products with high strength with sufficient plasticity and toughness, high resistance and small plastic deformations, brittle and fatigue fracture. Authors used flat specimens with a working part length and width of 100 mm and 200 mm, respectively. The thickness of the plates was 2 mm. The alloy under consideration is used in mechanical engineering, instrument manufacture and the tool industry. The chemical composition of the alloy and its physicomechanical characteristics are presented in the Table 1.

Table 1. Chemical composition and physicomechanical characteristics of titanium alloy.

Chemical composition of Titanium alloy							
Element	Ti	Al	Fe	O	Si	C	Other impurities
Mass fraction, %	99.3	0.18	0.17	0.15	0.08	0.06	0.06
Physicomechanical characteristics							
Characteristics	E		σ_B		δ_B		HB
Value	1.1 GPa		410 MPa		26%		150 MPa

Note: E – elasticity modulus; σ_B – tensile strength; δ_B – relative elongation at break; HB – Brinell hardness.

The purpose of the article is to describe the use of the hypothesis of linear damage summation when processing the results of fatigue tests. The objectives of the research are to determine the endurance limit of high strength material, as well as a mathematical measurement of the expected destruction.

2. Materials and methods

Fatigue tests of the pieces were carried out by the well-known methods (Korzhik, 1992c; Stepnov, 1985) on an electrodynamic shaker at normal temperature with cantilever mounting of the test piece (Figure 1). It is known that the work of external forces applied in the process of elastic deformation is conserved as some energy, which then restores the element after the stress is removed. However, when a crack appears in the material, the amount of elastic energy changes. If the elastic strain energy of a plate without a crack at a given stress level is equal to U_0, then in the presence of a crack it will be determined by the equation (Stepnov, 1985; Syrmanova et al., 2021):

$$U = U_0 - \frac{1}{E}\pi a^2 \sigma^2 + 4aT \tag{2}$$

where: E – elasticity modulus of the material; the component $\frac{1}{E}\pi a^2\sigma^2$ shows a decrease in the elastic strain energy of the plate due to the presence of a crack in it, *2a* is the crack length.

This expression was obtained under the assumption that in the presence of a crack of size 2a in the plate, the elastic energy of deformation is absent in the volume of the material equal to πa^2. The value $4aT$ – the surface energy of the crack, considering the formation of two surfaces; T – specific surface energy equal to the work required to form a unit area of the new surface. Initially, the total energy of the body increases with increasing crack length, which indicates that crack growth can occur only with increasing stresses. In this case, stable crack growth is observed. With an increase in the size of a crack to a certain critical size, the cracks grow due to the reserve of elastic energy without an additional increase in stresses (Korzhik, 1992a; 1992b; Khussain et al., 2022; Tokmuratov et al., 2020; Stepnov, 1985).

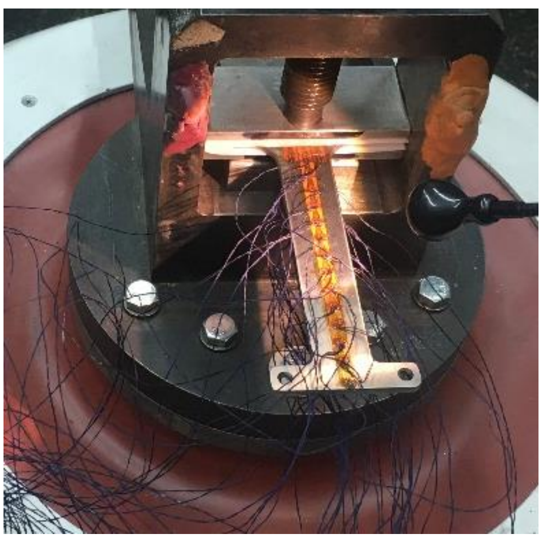

Figure 1. Photo of an electrodynamic shaker with a restrained test piece with strain gauges attached.

Indeed, the results of the study showed that at a stress level of σ_0 = 200 MPa along bending and torsional forms, crack formation processes were detected in the materials under study. At the same time, at the moment of the appearance of a crack in the specimen, a decrease in the frequency of natural vibrations by 3% was noted. Next, the fatigue curves for various fracture probabilities were analysed (Figure 2).

For the endurance limit, a level of vibration stresses was taken at which from 6 to 8 pieces passed (Antolovich & Armstrong, 2014; Stanzl-Tschegg, 2014). As can be seen from Figure 3, with the previously used approach to processing the results of fatigue tests, the endurance limit (based on 7 samples) practically lies on the fatigue curve with a fracture probability P = 0.5.

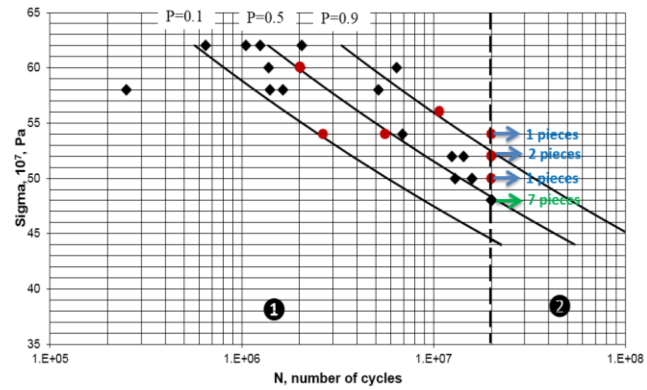

Figure 2. Fatigue curves for different fracture probabilities *P* (0.1; 0.5; 0.9).

Note: 1 – zone of failed test piece; 2 – zone of passed test piece; ◆ – pieces that failed at the one load level; ● – pieces that passed several load levels until the number of cycles to fracture was determined and then collapsed. Arrows indicate non-destroyed specimens.

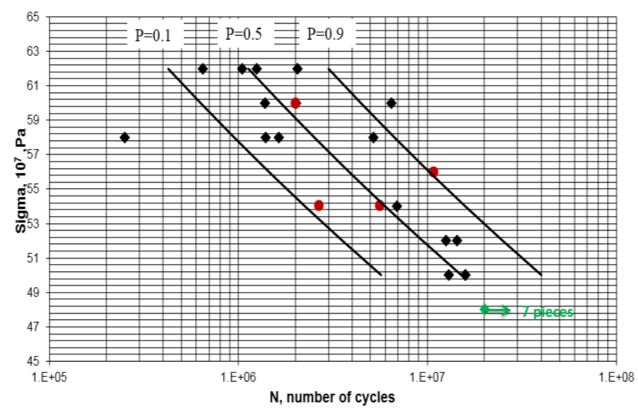

Figure 3. Fatigue curves for different fracture probabilities *P* (0.1; 0.5; 0.9).

3. Results and discussion

In the present study, the authors have carried out mechanical tests of materials for high-cycle fatigue with the number of load cycles up to 10^6-10^8. The amplitude for this type of test was selected in such a way that the material deformation occurred only in the elastic zone, and the stresses were less than the proportional elastic limit. The results of the study showed that the fatigue fracture observed in experiments has a complex development and depends on several factors (in this case, the composition and structure of the material, the load characteristics). The test data will be processed in 3 stages. At the first stage a regression analysis will be carried out, using only the durability at which the specimen fractured, the resulting fatigue curves are shown in the Figure 3.

The points corresponding to the specimens tested at several load levels are highlighted in red; only the last level at which the failure occurred is considered. The green dots corresponding to the endurance limit are not included in the analysis. At each *i*-th load level, after the number of cycles n_i, a certain fraction of fatigue damage ΔD_i was accumulated. Assume that the degree of breakdown is the same for all load levels and for each level of vibration stresses there is a limiting number of cycles-durability $N_i > n_i$, at which a crack (fracture) is likely to occur in the test piece (Borisov et al., 1986; Debroy et al., 2018; Kumar et al., 2017), then the damage accumulated at the level vibration stress $\boldsymbol{\sigma_i}$ is defined as:

$$\Delta D_i = n_i/N_i \tag{3}$$

At the final *k*-th the load level with the number of cycles n_k, a crack was formed in the test piece, which means that in accordance with the principle of linear damage summation, the damaging of the specimen accumulated at all levels reached its limiting value, taken equal to unity:

$$D_k = \sum_{i=1}^{k} \frac{n_i}{N_i} = 1 \tag{4}$$

To consider the fraction of accumulated damage at the load level passed by the specimen, Equation (1) is used, where the durability logarithm N_i is determined by the following equations:

$$Y_i = (Y_i)^{I}_{0.9} + s \tag{5}$$

where: $(Y_i)_{0.9}$ – the number of cycles corresponding to the quantile fatigue curve for the fracture probability $P = 0.9$ at the stress level $\boldsymbol{\sigma_i}$; s – a constant (yet unknown) coefficient for all load levels of a given test piece.

The coefficient s is determined by substituting Equation (5) into (4):

$$\sum_{i=1}^{k} \frac{n_i}{10^{lg(N_i)^{I}_{0.9}+s}} = 1 \tag{6}$$

where: n_1 – the number of cycles at the first (lower) stress level $\boldsymbol{\sigma_1}$ exceeding the material endurance limit, i.e., $\boldsymbol{\sigma_1 > \sigma_{-1}}$; $\boldsymbol{n_k}$ $n_k = N_k$ (failure at the *k*-th level), whence it follows the value:

$$s = lg\left(\sum_{i=1}^{k} \frac{n_i}{(N_i)^{I}_{0.9}}\right) \tag{7}$$

The second stage includes the determination of a certain equivalent durability (N_{eq}^{III}), to determine which the Equation (6) is used, presenting it in a slightly different form:

$$\frac{n_1}{10^{lg(N_1)^{I}_{0.9}+s}} + \sum_{i=2}^{k} \Delta D_i = \frac{n_1 + \Delta n_1^{II}}{10^{lg(N_1)^{I}_{0.9}+s}} = \frac{(N_1)^{III}_{eq}}{10^{lg(N_1)^{I}_{0.9}+s}} = 1 \tag{8}$$

where: Δn_1 – the number of cycles that the specimen would pass at the first level of vibration stresses before the cracks formation.

Equation (8) implies:

$$(N_1)^{III}_{eq} = 10^{lg(N_1)^{I}_{0.9}+s} \tag{9}$$

The third stage is carried out similarly to the first, with the replacement of the fatigue values for those obtained in the second stage, as well as with the exclusion of points with stress levels below the endurance limit (Hryhorenko et al., 2020; Liu et al., 2019; Zhurinov et al., 2020). The results of the regression analysis obtained during the third stage are shown in Figure 4. Test pieces for which the durability was recalculated are indicated by red dots. Thus, it turns out that the endurance limit $\boldsymbol{\sigma}$- 1 = 480 MPa, determined from 7 undestroyed specimens, lies much closer to the fatigue curve with a fracture probability $P = 0.1$. And with the probability of survival $P = 0.9$ based on tests $N = 2{\bullet}10^7$ cycles, the level of vibration stresses corresponds to $\boldsymbol{\sigma}$-1 = 470 MPa.

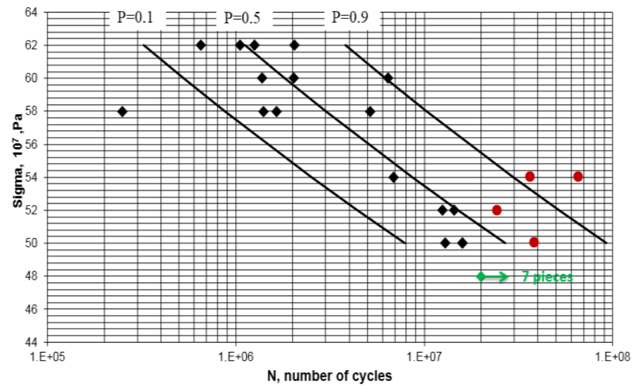

Figure 4. Fatigue curves for different fracture probabilities P (0.1; 0.5; 0.9) after linear damage summation.

To check the distribution of stresses in the sample and determine the localization of fractures, a calculation was performed for natural frequencies and modes of vibration with the determination of relative stresses in the samples using the ANSYS software package (Figure 5).

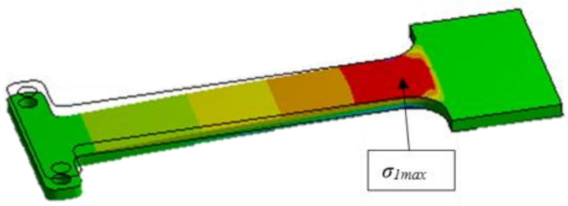

a)

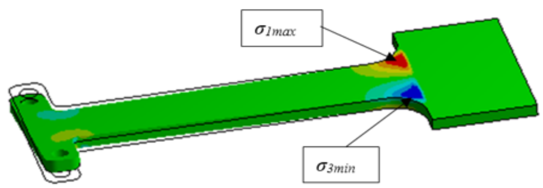

b)

Figure 5. Relative stress values for titanium alloy.

Note: a – when bending vibrations with a frequency f_1 = 213 Hz; *b* – when torsional vibrations with a frequency f_2 = 1515 Hz.

The simulation results made it possible to determine the places of localization of the maximum mechanical stresses arising under the considered loads and the loading scheme. Therefore, one should expect the occurrence of cracks in the regions with $\boldsymbol{\sigma}_{\max}$, (the regions in Figure 6 are highlighted in red). This is confirmed by the experiment, the results of which are shown in Figures 6, 7.

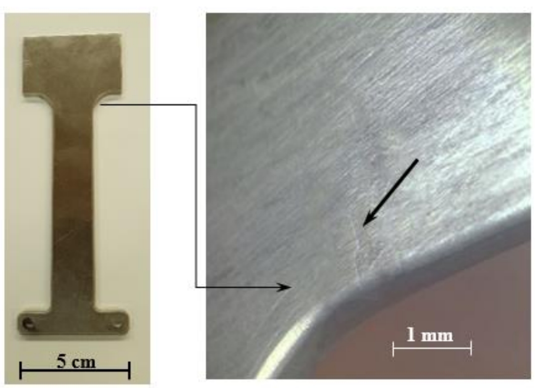

Figure 6. Failure of titanium alloy specimens after fatigue tests at resonant frequencies during bending vibrations.

Note: a – photo of the specimen; *b* – photograph of a sample section with a crack.

Figure 7. Micrograph of a crack after fatigue tests of a titanium alloy based on tests $N = 2{\cdot}10^7$ cycles with a vibration stress level $\boldsymbol{\sigma}_{-1}$ = 470 MPa.

The mechanism of fatigue fracture is largely associated with the inhomogeneity of the real structure of materials (difference in size, shape, orientation of adjacent metal grains) (Baishemirov et al., 2020; Chong et al., 2021; Grigorenko et al., 2019). The formation of cracks in the experiments began from the edge regions, which was confirmed by the results of scanning electron microscopic studies (Figure 8).

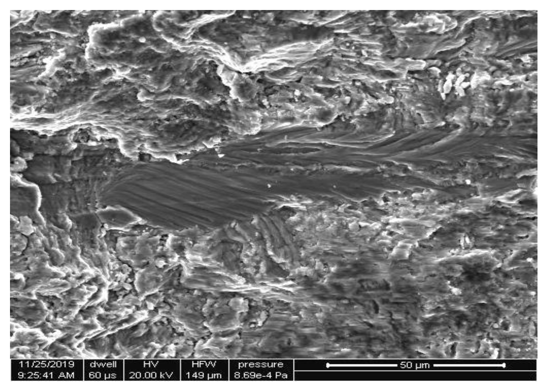

a)

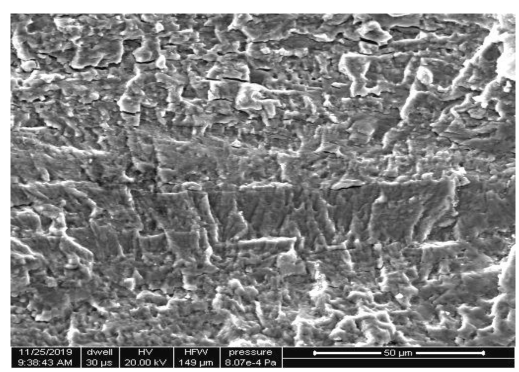

b)

Figure 8. Photography of fractured surfaces of a test piece.

Note: a – the initial stage of fatigue fracture; *b* – the final stage of fatigue fracture.

4. Conclusions

The presented results give grounds to conclude that the use of the hypothesis of linear summation of damages when processing the results of fatigue tests gives a satisfactory for practice accuracy of calculating the material fatigue limit. Thus, the results of the study showed that the hypothesis of linear damage summation is applicable for the material considered in question. From the analysis of the fatigue curves of the titanium alloy, it is shown that fracture occurs when the sample damage accumulated at all levels reaches its limiting value.

Also, the study did not reveal the effect of the sequence of stress and the loading history on the material durability. Experiments have shown that, as expected, a feature of the fracture process under cyclic loading is the appearance of microcracks in the material (long before fracture). Such microcracks were formed on the surface of the material where the change of the shape took place.

Conflict of interest

The authors do not have any conflict of interest to declare.

Funding

This study is conducted with financial support from the Ministry of Education and Science of the Russian Federation (project No. FZRR-2020-0023/code 0699-2020-0023).

References

Antolovich, S. D., & Armstrong, R. W. (2014). Plastic strain localization in metals: Origins and consequences. *Progress in Materials Science*, *59*, 1-160. https://doi.org/10.1016/j.pmatsci.2013.06.001

Baishemirov, Z., Tang, J.-G., Imomnazarov, K., & Mamatqulov, M. (2020). Solving the problem of two viscous incompressible fluid media in the case of constant phase saturations. *Open Engineering, 6*(1), 742-745. https://doi.org/10.1515/eng-2016-0100

Bekbauov, B., Berdyshev, A., Baishemirov, Z., & Bau, D. (2017). Numerical Validation of Chemical Compositional Model for Wettability Alteration Processes. *Open Engineering, 7*(1), 416-427. https://doi.org/10.1515/eng-2017-0049

Borisov, Y., & Korzhyk, V. (1998). Internal Stresses in Plasma Coatings with an Amorphous Structure. In *International Thermal Spray Conference 1998* (pp. 693-697). ASM International. https://doi.org/10.31399/asm.cp.itsc1998p0693

Borisov, Yu. S., Korzhik, V. N., Kunitskii, Ya. A., Revo, S. L., & Gritskiv, Ya. P. (1986). Structural transformations in thermal spray coatings of Ni60Nb40 alloy in vacuum annealings. *Soviet Powder Metallurgy and Metal Ceramics, 25*(10), 821-826. https://doi.org/10.1007/BF00801429

Borisov, Yu. S., Oliker, V. E., Astakhov, E. A., Korzhik, V. N., & Kunitskii, Yu. A. (1987). Structure and properties of gas-thermal coatings of Fe-B-C and Fe-Ti-B-C alloys. *Soviet Powder Metallurgy and Metal Ceramics, 26*(4), 313-318. https://doi.org/10.1007/BF01184439

Chong, Y., Bhattacharjee, T., Tian, Y., Shibata, A., & Tsuji, N. (2021). Deformation mechanism of bimodal microstructure in Ti-6Al-4V alloy: The effects of intercritical annealing temperature and constituent hardness. *Journal of Materials Science and Technology*, *71*, 138-151. https://doi.org/10.1016/j.jmst.2020.08.057

DebRoy, T., Wei, H. L., Zuback, J. S., Elmer, J. W., Beese, A. M., & Zhang, W. (2018). Additive manufacturing of metallic components – Process, structure and properties. *Progress in Materials Science*, *92*, 112-224. https://doi.org/10.1016/j.pmatsci.2017.10.001

Gates, N. R., & Fatemi, A. (2017). On the consideration of normal and shear stress interaction in multiaxial fatigue damage analysis. *International Journal of Fatigue*, *100*, 322-336. https://doi.org/10.1016/j.ijfatigue.2017.03.042

Grigorenko, G. M., Adeeva, L. I., Tunik, A. Y., Korzhik, V. N., & Karpets, M. V. (2020). Plasma Arc Coatings Produced from Powder-Cored Wires with Steel Sheaths. *Powder Metallurgy and Metal Ceramics, 59*(5-6), 318-329. https://doi.org/10.1007/s11106-020-00165-2

Grigorenko, G. M., Adeeva, L. I., Tunik, A. Y., Korzhik, V. N., Doroshenko, L. K., Titkov, Y. P., & Chaika, A. A. (2019). Structurization of Coatings in the Plasma Arc Spraying Process Using B4C + (Cr, Fe)7C3-Cored Wires. *Powder Metallurgy and Metal Ceramics, 58*(5-6), 312-322. https://doi.org/10.1007/s11106-019-00080-1

Hryhorenko, G. M., Adeeva, L. I., Tunik, A. Y., Karpets, M. V., Korzhyk, V. N., Kindrachuk, M. V., & Tisov, O. V. (2020). Formation of microstructure of plasma-arc coatings obtained using powder wires with steel skin and B4C + (Cr, Fe)7C3 + Al filler. *Metallofizika i Noveishie Tekhnologii, 42*(9), 1265-1282. https://doi.org/10.15407/mfint.42.09.1265

Khussain, B., Brodskiy, A., Sass, A., Yaskevich, V., Shlygina, I., Rakhmetova, K., Tungatarova, S., & Khussain, A. (2022). Research of the Thermal Effect on the Fe-Cr-Al Alloy Foil in the Initial State and with the Supported Secondary Carrier. *Coatings, 12*(9), 1266. https://doi.org/10.3390/coatings12091266

Korzhik, V. N. (1992a). Theoretical analysis of the conditions required for rendering metallic alloys amorphous during gas-thermal spraying. III. Transformations in the amorphous layer during the growth process of the coating. *Soviet Powder Metallurgy and Metal Ceramics, 31*(11), 943-948. https://doi.org/10.1007/BF00797621

Korzhik, V. N. (1992b). Theoretical analysis of conditions for metallic alloy amorphization on gas thermal deposition. 2. Phase formation under solidification of deposited material. Poroshkovaya Metallurgiya, (10), 11-15.

Korzhik, V. N. (1992c). Theoretical analysis of the amorphization conditions for metallic melts under gas-thermal spraying. I. Determination of cooling velocities of dispersed sprayed material. Poroshkovaya Metallurgiya, (9), 56-61.

Korzhyk, V., Khaskin, V., Grynyuk, A., Ganushchak, O., Peleshenko, S., Konoreva, O., Demianov, O., Shcheretskiy, V., & Fialko, N. (2021). Comparing Features In Metallurgical Interaction When Applying Different Techniques Of Arc And Plasma Surfacing Of Steel Wire On Titanium. Eastern-European Journal of Enterprise Technologies, 4(12-112), 6-17.

Kumar, S., Chattopadhyay, K., & Singh, V. (2017). Effect of ultrasonic shot peening on LCF behavior of the Ti–6Al–4V alloy. *Journal of Alloys and Compounds*, *724*, 187-197. https://doi.org/10.1016/j.jallcom.2017.07.014

Kunanbayeva, Y., Yerimbetov, B., Chalabayev, B., Aubakirova, F., & Duissenbekov, B. (2022). Application of Mixed Load-Bearing Structures in Earthquake Engineering. *Geotechnical and Geological Engineering, 40*(11), 5527-5537. https://doi.org/10.1007/s10706-022-02230-6

Kunitskii, Yu. A., Korzhik, V. N., & Nemirovskii, A. V. (1990). Transformations in the plasma-sprayed Fe67Ti7B24C2 alloy in heating. *Soviet Materials Science, 26*(1), 87-90. https://doi.org/10.1007/BF00734547

Kunitskii, Yu.A., Bespalov, Yu.A., Korzhik, V.N. (1988). Structural heterogeneities in amorphous materials from a Ni-Nb alloy. *Soviet Powder Metallurgy and Metal Ceramics, 27*(10), 763-767. https://doi.org/10.1007/BF00802767

Kvasnytskyi, V., Korzhyk, V., Kvasnytskyi, V., Mialnitsa, H., Dong, C., Pryadko, T., Kurdyumov, G. V., Matviienko, M., & Buturlia, Y. (2020). Designing brazing filler metal for heat-resistant alloys based on Ni3Al intermetallide. Eastern-European Journal of Enterprise Technologies, 6(12), 6-19.

Lei, M., Wang, J., & Yao, Y. (2021). A phase-transformation based method coupled with entropy to predict fatigue crack initiation of metallic materials. *Engineering Fracture Mechanics*, *250*, Article number 107757. https://doi.org/10.1016/j.engfracmech.2021.107757

Liu, C., Liu, D., Zhang, X., Ma, A., Ao, N., & Xu, X. (2019). Improving fatigue performance of Ti-6Al-4V alloy via ultrasonic surface rolling process. *Journal of Materials Science and Technology*, *35*, 1555-1562. https://doi.org/10.1016/j.jmst.2019.03.036

Mukhambetzhanov, S. T., & Baishemirov, Z. D. (2013). Procedure of evaluation development for drilling-in and well completion. World Appl Sci J, 24(2), 168-74.

Panfilov, M. B., Baishemirov, Z. D., & Berdyshev, A. S. (2020). Macroscopic Model of Two-Phase Compressible Flow in Double Porosity Media. *Fluid Dynamics, 55*(7), 936-951. https://doi.org/10.1134/S001546282007006X

Razavi, S. M. J., Ayatollahi, M. R., & Berto, F. (2020). Assessment of mixed mode fatigue crack growth under biaxial loading using an iterative technique. *Procedia Structural Integrity*, *26*, 240-245. https://doi.org/10.1016/j.prostr.2020.06.029

Rege, K., Gronsund, J., & Pavlou, D. G. (2019). Mixed-mode I and II fatigue crack growth retardation due to overload: An experimental study. *International Journal of Fatigue*, *129*, Article number 105227.
https://doi.org/10.1016/j.ijfatigue.2019.105227

Shojaei, A. K., & Volgers, P. (2017). Fatigue damage assessment of unfilled polymers including self-heating effects. *International Journal of Fatigue*, *100*, 367-376. https://doi.org/10.1016/j.ijfatigue.2017.03.017

Stanzl-Tschegg, S. (2014). Very high cycle fatigue measuring techniques. *International Journal of Fatigue*, *60*, 2-17.
https://doi.org/10.1016/j.ijfatigue.2012.11.016

Stepnov, M. N. (1985). *Static methods for processing the results of mechanical tests*. Mashinostroyeniye.
http://www.termist.com/bibliot/stud/stepnov/232.htm

Suleimenov, L., Zhangabay, N., Utelbayeva, A., Murad, M. A. A., Dosmakanbetova, A., Abshenov, K., Buganova, S., Moldagaliyev, A., Imanaliyev, K., & Duissenbekov, B. (2022). Estimation of the strength of vertical cylindrical liquidstorage tanks with dents in the wall. Eastern-European Journal of Enterprise Technologies, 1(7-115), 6-20.

Syrmanova, K. K., Alipbekova, Z. K., Suleimenov, U. S., Kaldybekova, Z. B., Kovaleva, A. Y., & Botashev, Y. T. (2021). Bitumen and asphalt concrete qualitative properties improvement depending on rubber crumb using. *Rasayan Journal of Chemistry, 14*(2), 778-784. https://doi.org/10.31788/RJC.2021.1426109

Tokmuratov, A. M., Dujsenbekov, B. K., Varenik, A. S., & Varenik, K. A. (2020). Dependencies of nonlinear hereditary creep theory for concrete and creep type equations of hardening under plane stress. *IOP Conference Series: Materials Science and Engineering, 939*(1), 012079.
https://doi.org/10.1088/1757-899X/939/1/012079

Zhurinov, M. Z., Abilmagzhanov, A. Z., Khussain, B. K., & Teltaev, B. B. (2020). Synthesis of anatase modification titanium dioxide nanopowders. *News of the National Academy of Sciences of the Republic of Kazakhstan, Series of Geology and Technical Sciences, 1*(439), 197-200.
https://doi.org/10.32014/2020.2518-170X.24